International Journal of Recent Technology and Engineering (IJRTE)
ISSN: 2277-3878, Volume-8 Issue-4, November 2019

Lung Nodule Detection: Image Enhancement using Fuzzy Rule Based Contrast Limited Adaptive Histogram Equalization and Entropy Weighted Residual Convolution Neural Network Method in CT

K.S. Gowri laksshmi, R.Umagandhi

***Abstract*— Computed Tomography (CT) images are read by several lung nodule detection methods. The early step of contrast enhancement is mandatory because of low contrast in original image and further techniques of image processing are with unsatisfactory results. Hence this process are resulted an enhanced image of clearly discrete lung area from background. Image enhancement, feature extraction, and classification are three primary steps. In this work, Rule based Contrast Limited Adaptive Histogram Equalization (FRCLAHE) perform image enhancement step followed by feature extraction and Fuzzy Rule (FR) determines the contrast value.**

From rules upper contrast value are determined then image is enhancement from CLAHE. In the second, the feature extraction is conducted using the Fuzzy Continuous Wavelet Transform (FCWT) and Gray Level Feature Extraction (GLCM). After this step, the classification is completed using the Entropy Weighted Residual Convolution Neural Network (EWRCNN). Finally, the results are evaluated between the samples, compared to FP reduction with Faster R-CNN alone, the inclusion of rule-based classification lead to an improvement in detection accuracy for the CAD system. These preliminary results demonstrate the feasibility of the proposed EWRCNN approach to lung nodule detection and FP reduction on CT images.

Keywords: lung Nodule Detection, T2-weighted MR images, Faster R-CNN, FP reduction, Fuzzy Rule based Contrast Limited Adaptive Histogram Equalization Fuzzy Continuous Wavelet Transform, Gray Level Feature Extraction, Entropy Weighted Residual Convolution Neural Network.

I. INTRODUCTION

A long and diligent development is done in the lung cancer screening with CT with critical milestones. the Centers for Medicare and Medicaid Services in November 2014 gives an statement on health and economic impacts about CT screening for lung cancer that in mid age of 55 and 74 years holding smoking habit of 30 pack-years must undergo lung cancer screening [1]. Since it is a leading cause of death, United States, Europe, and several other countries consider Lung cancer is a major problem to resolve. Early stage prediction and treatment are needed to prevail over this problem. Lung cancer diagnosis ie. to detect tumors are done by Computed Tomography (CT) ,a mass-screening tool. 20% of deaths are avoided at low-dose CT scans as per the National Lung Screening Trial result. But in future, CT examinations may increase for lung screening. Thus it generates more images that possibly read alone by radiologist for error free diagnostic reading.

Radiologists consider Computer-Aided Detection (CAD) for “second opinion” to diagnose several diseases from medical images. Several CAD methods prevail to detect the lung nodule. Image processing and machine learning approaches are developed by many researchers.

Aggarwal, Furquan and Kalra [2] developed for lung anatomy structure for classification linking nodules and normal. Characteristics like geometrical, statistical and gray level are distinguished. Segmentation is done by optimal thresholding and LDA is done by classifier. But it achieves accuracy of 84%, sensitivity of 97.14% and specificity of 53.33%. But its accuracy is in fluctuations in detecting the cancer nodule. Yet machine learning techniques and simple segmentation techniques are not doing classification hence incorporating the both techniques gives improvement probability of.

Jin, Zhang and Jin [3] developed a CAD system to detect the lung cancer using convolution neural network as classifier. It attains 84.6% of accuracy, 86.7% specificity and 82.5% of sensitivity. Circular filter is used in Region of interest (ROI) extraction phase for low cost training and recognition steps but fails to give satisfactory accuracy.

Sangamithraa and Govindaraju [4] developed a technique for clustering or segmentation based on K mean unsupervised learning algorithm. Certain characteristics cluster the pixel dataset.

Manuscript published on November 30, 2019.
* Correspondence Author
K.S. Gowri laksshmi, MSc, M.Phil, , Research scholar, Department of Computer Science, Kongunadu Arts and Science College, Coimbatore, Tamil Nadu 641029,India.(Email: gowrisasi2@gmail.com)
Dr.R.Umagandhi, MCA, M.Phil, PhD, Associate Professor and Head Department of Computer Technology, Kongunadu Arts and Science College, Coimbatore, Tamil Nadu 641029, India. .(Email: umakongunadu@gmail.com)

Back propagation network is used for classification here and gray-level co-occurrence matrix (GLCM) method extracts the features as entropy, correlation, homogeneity, PSNR, SSIM with its system accuracy of as 90.7%. Noise removal is done by Image pre processing median filter for enhancing new model to enhancing accuracy Roy, Sirohi, and Patle [5] designed using fuzzy interference system and active contour model a method to determine the lung cancer nodule. Image contrast enhancement is done by gray transformation. Segmentation is done after Image binarization and segmentation of resulted image are done by active contour model. Fuzzy inference method performs Cancer classification. The classifier is trained by features as area, mean, entropy, correlation, major axis length, minor axis. As a result, 94.12% accuracy is attained. Based on its limitation counting, further classification is done as cancer level.

Ignatious and Joseph [6] designed a watershed segmentation system. Image quality is enhanced by Gabor filter in pre-processing. It compares the accuracy with. 90.1% accuracy is attained in this model against neural fuzzy model and region growing method. Marker controlled watershed segmentation is implemented here for over segmentation problem but fails to classify the cancer level as benign or malignant and also reaching unsatisfactory accuracy.

Gonzalez and Ponomaryvo [7] developed a priori information and House field system for classification and the Region of Interest(ROI) calculated by Unit(HU). Extraction is done for area, eccentricity, circularity, fractal dimension and textural features like mean, variance, energy, entropy, skewness, contrast, and smoothness features are done and trained. The support vector machine classify and identify the benign nodule or malignant. Even it predicts and classify it fails in need of prior information of region interest.

Li et al. [8] developed a method for CT scans to check suspicious region as normal or nodule by shallow CNN. Image patches as nodule or normal are classified by three CNNs of various input sizes and depths [9]. For CT nodule detection, the two primary steps of deep learning based methods are proceeded. Extraction and cropping are done on first nodule candidate by a deep learning network. Different in lung nodule size, fixed cropping of each region is not suitable reason. Hence to resolve Faster R-CNN is implemented for lung nodule detection in [10]. the whole image is fed as input without candidate extraction in Faster R-CNN and detects lung nodules of various sizes as multiple anchors entry. a spatial three-channel input is added to add spatial information in the input image. Over fitting may overcome by transfer learning in parameter optimization. But it leads in low contrast and need further contrast enhancement.

With above said pitfalls of existing methods, CT Images are segmented using of Fuzzy Rule based Contrast Limited Adaptive Histogram Equalization (FRCLAHE) for image enhancement and Entropy Weighted Residual Convolution Neural Network (EWRCNN) based Detection hence. The proposed plan has sequence steps as preprocessing, removal of noise in input images and extraction of feature and gray level by Fuzzy Continuous Wavelet Transform feature. Afterward Fuzzy Rule based Contrast Limited Adaptive Histogram Equalization is done for image enhancement before nodule detection and feature extraction. Thence the lung area is distinguished from background and classification of lung nodules are attained from enhancement image by the Entropy Weighted Residual Convolution Neural Network (EWRCNN) classifier. Intensity, shape (2D and 3D) and texture features are selected for optimization of sensitivity by reducing the false positives. Additionally, performance comparison is done by EWRCNN and Faster R-CNN. Therefore, the visibility of nodule in lung field is improved by proposed results. Fig.1 explains the overall architecture.

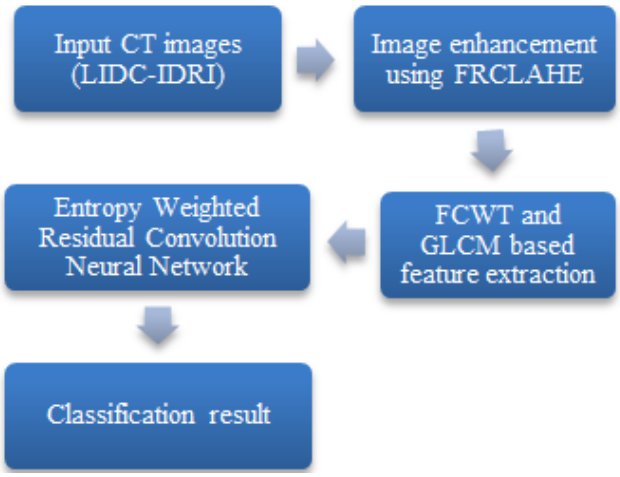

Fig.1.Architecture diagram of Proposed Lung Nodule Detection System

The rest of this work is organized as follows: Section 2 presents the dataset description and the proposed Entropy Weighted Residual Convolution Neural Network method in detail. Experimental setup and Results comparisons are given in Section 3. Conclusions and future work are summarized in Section 4.

II. LUNG NODULE DETECTION

2.1 DATASET

Lung Image Database Consortium image collection (LIDC-IDRI) inclusive of diagnostic and lung cancer screening thoracic computed tomography (CT) scans with marked-up annotated lesions are taken as dataset. Computer-assisted diagnostic (CAD) method, a web-accessible international resource is considered for development, training, and evaluation for lung cancer detection and diagnosis. It is originated by the National Cancer Institute (NCI), later developed by the Foundation for the National Institutes of Health (FNIH), and convoyed through active participation by the Food and Drug Administration (FDA). The success of a consortium founded on a consensus-based process are determined by this public-private partnership demonstrates. This data set inclusive of 1018 cases is created by seven collaborated academic centers and eight medical imaging companies. The results of a two-phase image annotation process performed by four experienced thoracic radiologists are recorded from a clinical thoracic CT scan and an XML file on every subject.

Three categories are determined for the initial blinded-read phase by each radiologist independently reviews as "nodule > or =3 mm," "nodule <3 mm," and "non-nodule > or =3 mm". The quality of the CT image is improved by forthcoming image enhancement phase. Fig. 5 represents the data set image with 512*512 LIDC-IDRI images.

2.2 Image Enhancement

The CT images are mainly focused in the scanning and medical field. Such images are enhanced by various techniques for further study. Several image enhancement techniques and algorithms exist but fail to have good result and common technique for enhancing all sort of CT image in medical image or scan image. Hence, Fuzzy Rule based Contrast Limited Adaptive Histogram Equalization (FRCLAHE) is proposed to tackle this problem with base of image enhancement theory. When an area of the image is of specific crucial with changes in pixel intensity FRCLAHE contrast enhancement is used.

If the image is being displayed on a low quality screen prediction by the human eye is difficult to make out the clear structures. By exaggerating interpretation of the image is easier if the changes in pixel intensity are exaggerated. the readability of areas with subtle changes are improved by the CLAHE but if intensity of the pixels is outside the range of intensities being enhanced are wiped out the image area. The image processing is done efficiently by the fuzzy rule-based approach. A simple inference rule-based system is developed in this proposed work with four phases. As a first phase, initialization the image parameters are done. Following to that, sets of gray levels are done by Fuzzification in gray levels phase (i.e., membership values to the dark, gray and bright. Sequentially gray level modification phase is done before the final defuzzification phase.

Initialization of Parameter: As starting phase, the image parameters are initialized by determining the maximum (max) and minimum (min) gray levels and find out the mid gray levels. Clipping limit helps to amplify the histogram of an image with specific value called as CLAHE limits. This clipping level determines the value of noise in the histogram to be smoothened & determines the contrast of the image to be enhanced and apply histogram clip (HC). The over-enhancement of image background regions is controlled and clipping level is adjusted by the CLAHE. Contrast is one of property determines the quality depending upon the pixel intensity as:

$$Contrast = \frac{Object - Background}{Background}$$

hence block size determines the concept and the quality of results of CLAHE are controlled by clip limit.

Phase of Fuzzification Process: Fuzzification of the gray levels is the second phase of the algorithm (dark, gray and bright are membership values). An array of fuzzy singletons with *I image size* of *M* x *N* and L gray levels are taken with membership value representing its degree of brightness accordingly on some brightness levels.

$I = \bigcup_{mn} \frac{\mu(g_{mn})}{g_{mn}} \forall m = 1,2,\dots,M$ and $n = 1,2,\dots,N$, is calculated for an image *I*, of fuzzy sets while g_{mn} represents $(m,n)^{th}$ pixel intensity and membership value by μ_{mn}. The apt image property like its edge, dark, textural property is characterized by the membership function and it is defined as whole image globally or segmented image locally. Additionally, the inference mechanism is done by gray level modification.

Phase of Defuzzification Process: the new enhanced gray level as defuzzification of output is calculated as using minimum ($gray_{min}$), maximum ($gray_{max}$) and medium ($gray_{mid}$) of the gray levels as

$$g = \frac{\mu_{dark} * gray_{min} + \mu_{gray} * gray_{mid} + \mu_{bright} * gray_{max}}{\mu_{dark} + \mu_{gray} + \mu_{bright}}$$

hidden area are enhanced by FRCLAHE image pre-processing, CLAHE method's clipping factor selection, various image touch by fuzzy approach, sharpens the lung nodules edges inside the image and its image contrast identifies lung nodule effectivly.

2.3 Feature Extraction

Automatic feature extraction from biomedical images and successive classification are explained in this subsection. The spatial orientation of high-frequency image and textural features of the processed image are exploited by a two-step process. Initially, the HH high-frequency sub band image are obtained by the Fuzzy Continuous Wavelet Transform and sub-band images are extracted with its texture features by GLCM. Sub-images of 3 × 3 divisions are taken as input for GLCM algorithm. Using of mat lab Contrast, Inverse Difference Moment, Entropy, Energy, Sum

average and two values of Homogeneity are the extracted seven features from GLCM as computed by Soh and Tsatsoulis [11].

The total number of features "values" per image in GLCM method is computed using the following equation:

Number of features (GLCM) = number of directions (directions = 3) × 0.5 × d × number of extracted features (GLCM) × numberof subimages.

Thus produce either Feature Vector (F_V) is subsequently fed to the proposed classifier to classify normal versus pathological images. The feature extraction stage is clearly shown in Fig.2

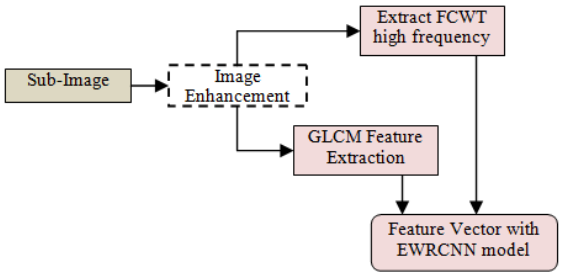

Fig.2.The Structure of feature extraction method

2.4 Lung Nodule Detection

2.4.1 FASTER R-CNN

Two modules are handled in Faster R-CNN [12]. As initial module RPN produce every image including proposed regions. As Fast R-CNN detector is secondary module perform classification among the regions.

convolutional layers are being shared by RPN and Fast R-CNN for time consumption. The initial of 3 × 3 convolutional layer are the convolution layers of a pre-trained network in RPN.

Sequentially, classification and regression add two 1 × 1 convolutional layers accordingly. Set up the anchors and get associate to deal with various aspect ratios and scales of lung nodules in the RPN. 3 scales (128 × 128, 256 × 256 and 512 × 512 pixels) and 3 aspect ratios (1: 1, 1: 2, and 2: 1) are the default setting of anchors, with k = 9 anchors at every location. Fig.5 explains that the adjustment of anchor scale is done for nodule occupying a minimal area in the image. To train the feature extraction model and its parameters for over fitting by direct use of CT images. Hence the features are extracted using FCWT-GLCM at initial to overcome these pitfalls. Further, the initial parameters are considered with a pre-trained model from natural images and then the final parameters value are received in sequential fine-tune. The two labels are consigned to every anchor the Region Proposal Network training where T2W-CT slice is one channel gray level image. The nodule region is determined by its positive label. Negative label is determined at non-overlap with its assigned ground-truth box and is considered as the normal region.

Positive label are assigned with two kind of anchors as

1. Maximum Juncture-over-Merger (JoM) overlap in the anchor with the with a ground truth box.
2. A JoM overlaps higher than 0.6 with any ground-truth box in the anchor.

Classification loss LF_{cls} and regression loss L_{reg}. Are the two Loss Function (LF) of RPN for an image as

$$LF(\{p_i\},\{t_i\}) = \frac{1}{N_{cls}}\sum_i LF_{cls}(pp_i, pp_i^*) + \lambda\frac{1}{N_{reg}}\sum_i pp_i^*\, LF_{reg}(pbb_i, pbb_i^*)$$

index of the anchor is i, the predicted probability of anchor i being a lung nodule is pp_i, the ground truth label for anchor i is pp_i^*. $pp_i^* = 1$ and $pp_i^* = 0$ is present if anchor i is positive and negative accordingly. $[pbb_x, pbb_y, pbb_w, pbb_h]$ and $[pbb_x^*, pbb_y^*, pbb_w^*, pbb_h^*]$. are the is the predicted bounding box of pbb_i $and\ pbb_i^*\ of$ positive anchor. LF_{cls} is the loss function of classification for two classes, defined as: $LF_{cls}(pp_i,) = pp_i^* - log[p_i p_i^* + (1 - pp_i^*)(1 - pp_i)]$

In above equation, LF_{reg} is the loss function for regression, defined as: $LF_{reg}(pbb_i, pbb_i^*) = \sum_i smooth_{LF1}(pbb_i - pbbi*)$ here, $smoothLF1$ is defined as follows.

$$smooth_{LF1}(x) = \begin{cases} 0.5x^2 & if\ |x| < 1 \\ |x| - 0.5 & otherwise \end{cases}.$$

The classification loss and the regression loss are normalized by $N_{LF_{cls}}$ and $N_{LF_{reg}}$ and weighted by parameter λ. The four coordinates for pbb_i and pbb_i^* are as follows:

$pbb_x = \frac{x - x_a}{w_a}, pbb_y = \frac{y - y_a}{h_a}, pbb_w = log\left(\frac{w}{w_a}\right), pbb_h = log\left(\frac{h}{h_a}\right), pbb_x^* = \frac{x^* - x_a}{w_a}, pbb_y = \frac{y^* - y_a}{h_a}, pbb_w^* = log\left(\frac{w^*}{w_a}\right), pbb_h^* = log\left(\frac{h^*}{h_a}\right)$. In above equation x, y is the box's center coordinates w is width and h denote height.x, x_a andx^* are for the predicted box, anchor box, and ground-truth box respectively (likewise for y; w; h). Thus the output of Faster R-CNN is the predicted nodule position and the probability of being a nodule.

the region proposals output from RPN is inaccurate is major disadvantage with Faster R-CNN architecture because of some hard coded anchors with fixed scales and aspects in RPN according to the potential regions. If bounding box regression part is detected RPN tries lung nodules segmentation but fails to give accuracy in lack of specific class knowledge. Bounding box regression fails on classification error and proposed region error. Hence proposed regions are finer, final bounding box regression is improved and so achieves high accuracy by Entropy Weighted Residual Convolution Neural Network Method is further improved if the and it is achieved.

2.4.2 Proposed Entropy Weighted Residual Convolution Neural Network Method

At origin phase, the lung nodule region as the lung nodule region is not completely utilized as regressed bounding box is one of the outputs by Faster R-CNN network. on the other hand, lung nodule as finer bounding box is iterated of classification and bounding box regression of prior output using the regressed bounding. It is done as the plotting the defected lung nodule and being iterated still refinement of the region as nodule detection result are attained. Fig.3 shows the model of entropy weighted residual CNN. feature extraction phase perform feature extraction as Faster R-CNN as in the first iteration, region proposals are obtained from RPN and cropping and resizing of new feature maps are done by RoI pooling layer and final class scores and bounding box regression for each class are obtained using a three-layer Fully Connected (FC) network. The first iteration gets over on proposed region and regressed bounding box with the maximum class score are select taken as region proposal of the second iteration and being of CT images. Recalculation is not necessary for RoI pooling layer input in reusing of feature maps. In all iterations, FC network uses parameter of the three-layer. Repeat this process for forthcoming iterations also. In Fig.3 iteration number as 3 taken and the feature maps extraction and each initial RPN region proposal are calculated as.

$FV = feature\ extraction(image)$, $RP_1 = RPN(FV)$

T is set iteration number and for each iteration i, the model can be represented as

$$for\ i = 1, 2, \ldots T,\begin{cases} r_i = RoIP\ ooling(F_V, RP_i) \\ scores_i, boxes_i = FC^3(r_i) \\ H_\alpha(F_V) = S_\alpha(A_1, A_2, \ldots A_C) \\ RP_{i+1} = boxes_{i, arg\max j\in\{0\ldots C\}\, scores_{ij}} \\ loss_i = loss_{cross-entropy}(scores_i, c_i) + \\ \lambda[c_i \neq bg_i] loss_{smoothL1}(boxes_i, bg_i) \end{cases}$$

the three-layer fully connected network is denoted by FC^3, class label c_i for the proposed region RP_i for C the number of classes and bg_i denotes the ground truth bounding box of object in this region, $[c_i \neq$

$bg_i] = 1$ if the region selected is not background inclusive of object, otherwise $[c_i \neq bgi = 0$, and λ is the weight parameter to balance classification loss and bounding box regression loss. Renyi's α-entropy functional estimator [13] of matrix-based and its multivariate extension are exposed in this section. For a set of classesc_i, weighted entropy for a random variable X with Probability Density Function (PDF) f(x) in a finite set X(denoted as F_V),$H_\alpha(F_V)$ is defined as:

$$wH_\alpha(F_V) = \frac{1}{1-\alpha} log \int_x P_n F_V^{\ \alpha}(x)dx$$

The number of weights in the range values for classesc_i is represented by P_n .

Estimation of entropy, joint entropy for two or more variables directly from data without PDF estimation are carried out by Renyi's entropy in terms of the normalized Eigen spectrum of the Hermitian matrix of the projected data in Replicating Kernel Hilbert Space (RKHS). Given a collection of nCT images $\{(x_1^i, x_2^i, \dots, x_C^i)\}_{i=1}^n$, where the superscript i the image class label, each contains $C(C \geq 2)$measurements $x_1 \in X_1, x_2 \in X_2, \dots, x_c \in X_c$ obtained from the same realization, and the positive definite kernels $\varkappa_1: X_1 \times X_1 \to \mathbb{R}$, a matrix-based analogue to Renyi's α -entropy among C variables can be defined as:

$$S_\alpha(A_1, A_2, \dots A_C) = S_\alpha\left(\frac{A_1 \circ A_2 \circ \dots \circ A_C}{tr(A_1 \circ A_2 \circ \dots \circ A_C)}\right)$$

In above equation, $(A_1)_{ij} = \varkappa_1(x_1^i, x_1^j), (A_2)_{ij} = \varkappa_2(x_2^i, x_2^j), \dots, (A_C)_{ij} = \varkappa_k(x_C^i, x_C^j)$ and $\circ$ denotes the Hadamard product.

smooth L_1 norm loss is used for the bounding box regression and soft maxcross entropy loss is used for classification in training [19] and for every iteration, $loss_i$ is calculated. The total of all iterations are termed as final loss (additionally RPN loss). The final output is determined by the scores and bounding boxes of last iteration as

the final output: $\begin{cases} loss_{final} = \sum_{i=1}^{T} loss_i \\ output = scores_T, boxes_T \end{cases}$

Only one region proposal are given in above output. At origin if K region are yielded by RPN it is iterated for every proposal, and final loss is as average $loss_{final}$ of all K proposals.

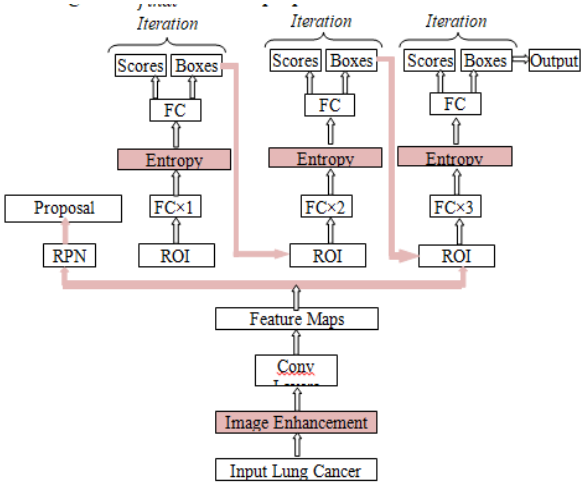

Fig.3. Architecture of Entropy Weighted Residual Convolution Neural Network

Endurance of lung parenchymas present in CT slice is not enough. Hence segmentation method for a rough lung parenchyma is implemented. Segmentation of thorax is done initially and then extraction of the lung parenchyma candidate in each slice is done. At last 3D connected component labeling do removal of the non-lung parenchyma tissues.

III. EXPERIMENTAL RESULTS AND DISCUSSION

The experimental results of proposed EWRCNN are evaluated and the performance results are compared with existing Faster RCNN and RCNN image compression schemes. Peak Signal to Noise Ratio (PSNR), Correlation, structural similarity (SSIM), Execution Time and Mean Square Error (MSE) are the parameters taken.

CT image: CT scans for diagnostic and lung cancer screening with marked-up annotated lesions are presented in the real time Lung Image Database Consortium image collection (LIDC-IDRI). 1018 cases in the dataset are considered in collaborated seven academic centers and eight medical imaging companies. Four experienced thoracic radiologists consider the X-ray image and its associated XML file, a clinical thoracic CT scan on each subject of for the results of a two-phase image annotation process. In starting phase of reading blindly, CT scan and marked lesions are reviewed by radiologist and said as among three categories (nodule>=3mm, nodule<3mm and non-nodule>=3mm). Fig.4 shows the result of CT-image with the nodule detection by proposed EWRCNN and existing Faster RCNN. The results evaluation results for the corresponding three methods are shown in fig 6-9. The overall results are given in Table 1 for CT.

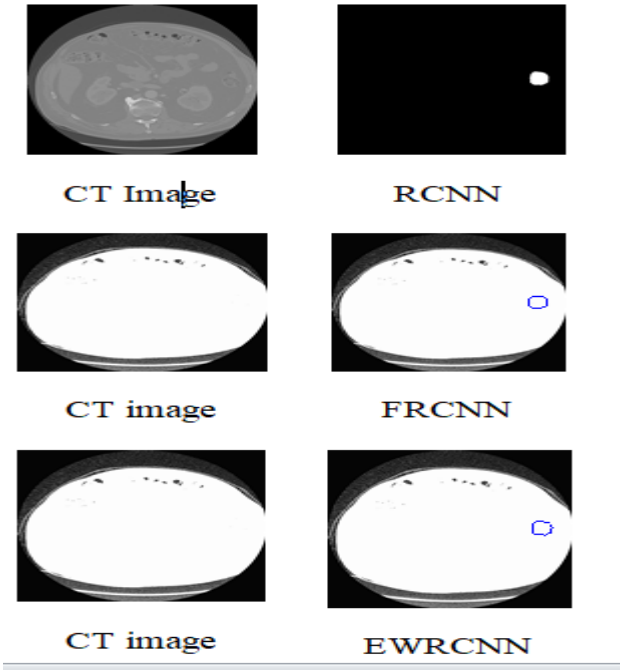

Fig.4. lung nodule detection in CT image and its classification results

Table 1. Lung nodule detection in CT image and its classification results

	RCNN classification	Faster RCNN classification	EWRCNN Classification
Accuracy	81.0307	88.6204	91.9346
Precision	51.2075	52.2499	53.1950
Recall	81.1222	88.8299	91.3062
F- Measure	62.7836	65.7976	67.2248

Precision Result comparison

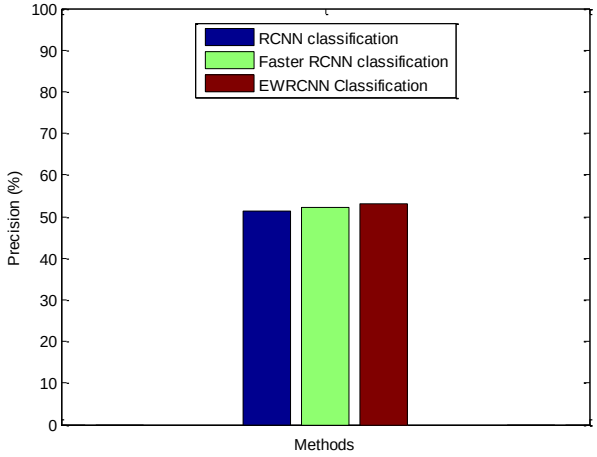

Fig.5. Comparison of compression techniques in Precision

The results of correlation comparison between proposed EWRCNN, and existing Faster RCNN and RCNN are shown in Fig.5. From the figure, the proposed method can obtain high precision rate against existing methods. the high precision rate of 53.1950 is achieved by this effective way in lung nodule. When comparing the precision among the existing methods are providing good precision rates, which is lower than the EWRCNN. The result exhibits proposed plan gives 0.9451 and 1.9875 better against existing methods such as Faster RCNN and RCNN respectively.

F-measure Result Comparison

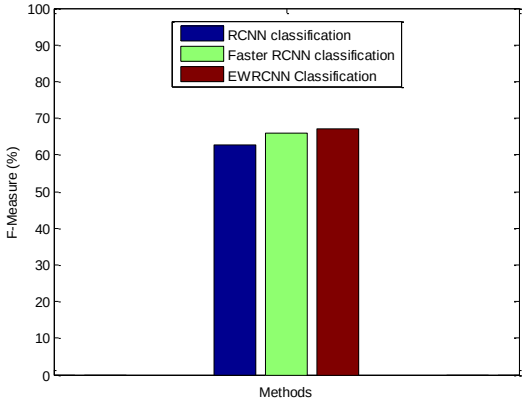

Fig.6. Comparison of compression techniques in F-measure

The F-measure comparison results between proposed EWRCNN, and existing Faster RCNN and RCNN are shown in Fig.6. The proposed method has high value of F-measure 67.2248. From the results, it is well know that proposed EWRCNN obtain high F-measure indicating the good lung nodule detection. Because, proposed plan is with base of excellent feature extraction and the entropy weighted based concept is enhancing the learning efficiency. When comparing the F-measure rate among the existing methods such as Faster RCNN and RCNN are providing fewer rates of 65.7976 and 62.7836 respectively, which indicates the proposed work can give better detection results than the existing methods.

Recall Result Comparison

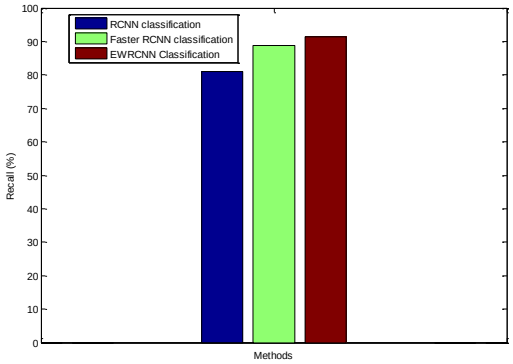

Fig.7 Comparison of compression techniques in Recall

The recall results against proposed EWRCNN, and existing Faster RCNN and RCNN are shown in fig.7. The proposed method has high value of recall rate of 91.3062. From the results, it is well know that proposed EWRCNN obtain high recall rate value indicating the good detection rate. Because, the proposed scheme is having the effective image enhancement stage which reduce the noises. When comparing the recall rate among the existing methods such as Faster RCNN and RCNN, providing recall rate of 88.6299 and 81.1222 respectively, which shows the proposed work can give better detection results than the existing methods.

Accuracy Result Comparison

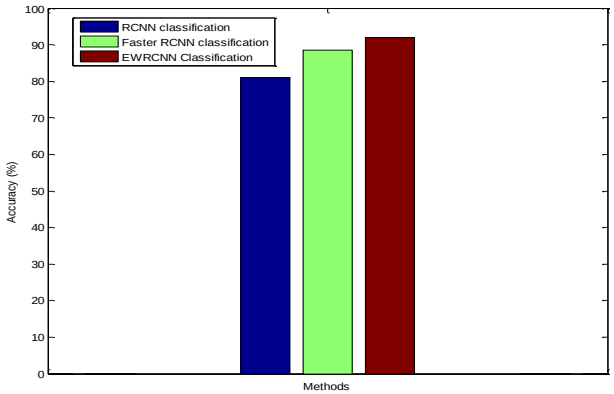

Fig.8 Comparison of compression techniques in Accuracy

The accuracy comparison results between proposed EWRCNN, and existing Faster RCNN and RCNN are shown in Fig.7. From the results, the proposed method attains high accuracy against existing methods. Efficient way of getting the lung nodule accuracy is reached as 91.9346 in proposed.

When comparing the accuracy among the existing methods such as Faster RCNN and RCNN providing less rate of 88.6204 and 81.0307 respectively. In above experimental results, the proposed work gives better against existing methods.

X-ray image: Fig.9 exhibits the results of real time X-ray image with the nodule detection .The results evaluation results for the corresponding three methods such as proposed EWRCNN, existing Faster RCNN and RCNN are shown in fig 9-11. Figure predicts that proposed system achieves higher efficiency of precision, f-measure and accuracy. The total results of X-ray images are tabulated in Table 2.

Table 2. Lung nodule detection of X-ray image with overall classification results for

	RCNN classification	Faster RCNN classification	EWRCNN Classification
Accuracy	82.1697	88.8420	91.7606
Precision	54.0634	56.8071	59.1270
Recall	82.2910	88.7729	91.8621
F- Measure	65.2554	69.2805	71.9460

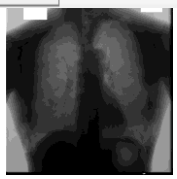

X-ray Image

Segmentation result

Fig.9. X-ray image for lung nodule detection in overall classification results in

IV.CONCLUSION

An initial step of contrast enhancement is mandatory because of image processing techniques leading in undesired results as original image are in low contrast. Enhanced image is seen with the lung area has crystal clear view on its background. With this motivation of work based on deep learning, a lung nodule detection method is developed for thoracic MR images. Here, the image enhancement is performed initially using Fuzzy Rule based Contrast Limited Adaptive Histogram Equalization (FRCLAHE) and then feature extraction is conducted using the Fuzzy Continuous Wavelet Transform (FCWT) and gray level feature extraction (GLCM). After this step for detecting lung nodule, the classification is completed using the Entropy Weighted Residual Convolution Neural Network (EWRCNN). As less dependent on scaling, candidate extraction could be avoided by this detection scheme. Many FP regions are existed and detected in the results as Faster R-CNN without involving anatomical characteristics. The tested result exhibits the Faster R -CNN detecting many nodules and reducing the FP regions by proposed EWRCNN. Furthermore it is

focused on reducing the number of false positives, increasing algorithm sensitivity, improving and optimizing the algorithm detection by considering the different sort of nodules on variety of sizes and shapes and at last, integrating ability with the Electronic Medical Record Systems and Picture Archiving and Communication Systems. Furthermore this analysis is enhanced to develop methodology to overwrite the above said pitfalls.

REFERENCES

1. Rubin, Geoffrey D. "Lung nodule and cancer detection in CT screening." Journal of thoracic imaging 30, no. 2 (2015): 130.
2. Aggarwal, T., Furqan, A., &Kalra, K. (2015) “Feature extraction and LDA based classification of lung nodules in chest CT scan images.” 2015 International Conference On Advances In Computing, Communications And Informatics (ICACCI), DOI: 10.1109/ICACCI.2015.7275773.
3. Jin, X., Zhang, Y., & Jin, Q. (2016) “Pulmonary Nodule Detection Based on CT Images Using Convolution Neural Network.” 2016 9Th International Symposium On Computational Intelligence And Design (ISCID). DOI: 10.1109/ISCID.2016.1053.
4. Sangamithraa, P., &Govindaraju, S. (2016) “Lung tumour detection and classification using EK-Mean clustering.” 2016 International Conference On Wireless Communications, Signal Processing And Networking (Wispnet). DOI: 10.1109/WiSPNET.2016.7566533.
5. Roy, T., Sirohi, N., &Patle, A. (2015) “Classification of lung image and nodule detection using fuzzy inference system.” International Conference On Computing, Communication & Automation. DOI: 10.1109/CCAA.2015.7148560.
6. Ignatious, S., & Joseph, R. (2015) “Computer aided lung cancer detection system.” 2015 Global Conference On Communication Technologies (GCCT), DOI: 10.1109/GCCT.2015.7342723.
7. Rendon-Gonzalez, E., &Ponomaryov, V. (2016) “Automatic Lung nodule segmentation and classification in CT images based on SVM.” 2016 9Th International Kharkiv Symposium On Physics And Engineering Of Microwaves, Millimeter And Submillimeter Waves (MSMW). DOI: 10.1109/MSMW.2016.7537995.
8. C. Li, G. Zhu, X. Wu, et al., “False-Positive Reduction on Lung Nodules Detection in Chest Radiographs by Ensemble of Convolutional Neural Networks,” IEEE Access, vol. 6, pp. 16060-7, 2018.
9. Li, Yanfeng, Linlin Zhang, Houjin Chen, and Na Yang. "Lung Nodule Detection with Deep Learning in 3D Thoracic MR Images." IEEE Access (2019).
10. Kim, Seung Jong, ByongSeok Min, Dong Kyun Lim, and Joo Heung Lee. "Determining Parameters in Contrast Limited Adaptive Histogram Equalization." (2013).
11. Soh, L-K., and Costas Tsatsoulis. "Texture analysis of SAR sea ice imagery using gray level co-occurrence matrices." IEEE Transactions on geoscience and remote sensing 37, no. 2 (1999): 780-795.
12. S. Ren, K. He, R. Girshick, et al., “Faster R-CNN: towards real-time object detection with region proposal networks,” IEEE Trans.Pattern Anal. Mach. Intell., vol. 39, no. 6, pp. 1137-1149, 2017.
13. M. M¨uller-Lennert, F. Dupuis, O. Szehr, S. Fehr, and M. Tomamichel, “On quantum r´enyi entropies: A new generalization and some properties,” J. Math. Phys., vol. 54, no. 12, p. 122203, 2013..